AN UPPER BOUND FROM HELIOSEISMOLOGY ON THE STOCHASTIC BACKGROUND OF GRAVITATIONAL WAVES

Daniel M. Siegel[1] and Markus Roth[2]
Draft version April 1, 2014

ABSTRACT

The universe is expected to be permeated by a stochastic background of gravitational radiation of astrophysical and cosmological origin. This background is capable of exciting oscillations in solar-like stars. Here we show that solar-like oscillators can be employed as giant hydrodynamical detectors for such a background in the μHz to mHz frequency range, which has remained essentially unexplored until today. We demonstrate this approach by using high-precision radial velocity data for the Sun to constrain the normalized energy density of the stochastic gravitational-wave background around 0.11 mHz. These results open up the possibility for asteroseismic missions like *CoRoT* and *Kepler* to probe fundamental physics.

Subject headings: asteroseismology — gravitational waves — stars: oscillations (including pulsations) — Sun: helioseismology — Sun: oscillations

1. INTRODUCTION

A stochastic background of gravitational waves (SBGW) is expected to result from the incoherent superposition of gravitational radiation from a large number of sources (Maggiore 2000; Sathyaprakash & Schutz 2009). It can be subdivided into a cosmological background of primordial gravitational waves (GWs) generated by processes of the very early universe, and into an astrophysical background produced by a large number of unresolved astrophysical sources that consist of an accelerated mass distribution with a quadrupole moment. Many potential processes of the very early universe have been proposed as generators of cosmological SBGWs, examples of which are standard inflationary models, pre-Big-Bang models, and cosmic strings (Maggiore 2000). Candidate sources to produce the astrophysical component are, for instance, compact binary star systems, core collapse supernovae, and rotating neutron stars (Schneider et al. 2010; Regimbau 2011; Amaro-Seoane et al. 2013). Since the universe has been essentially transparent to gravitational radiation from the very beginning, GWs are ideal carriers of information on the physical processes that generated them and thus on the state of the universe at the time they were produced. This background encodes information on the very early epoch as well as on the more recent history of the universe that is not accessible to conventional astronomical observations based on electromagnetic waves (Maggiore 2000; Sathyaprakash & Schutz 2009; Schneider et al. 2010; Hils et al. 1990). Extracting this astrophysical and cosmological information from the SBGW and thus disentangling the various contributions requires GW experiments in a variety of frequency bands.

Tight upper bounds on the SBGW have been placed at high and low frequencies by Earth-based interferometric detectors such as LIGO (around 100 Hz; Abbott et al. 2009), pulsar timing observations based on the residuals of pulse arrival times (between $10^{-9} - 3 \times 10^{-8}$ Hz; Jenet et al. 2006), and cosmic microwave background (CMB) observations at large angular scales which indicate an upper limit on the cosmological component of the SBGW at larger wavelengths than the horizon size at the time the CMB was produced ($3 \times 10^{-18} - 10^{-16}$ Hz; Maggiore 2000). However, the intermediate frequency regime between $10^{-8} - 10$ Hz has proven to be particularly challenging to be probed by GW experiments and has thus remained essentially unexplored until today. Apart from the frequency-independent indirect limits from CMB and Big-Bang nucleosynthesis (BBN) data (Smith et al. 2006; Cyburt et al. 2005), which only place tight bounds on the cosmological component of the SBGW, there are limits from Doppler tracking of the Cassini spacecraft ($10^{-6} - 10^{-3}$ Hz; Armstrong et al. 2003), from precision orbital monitoring of the Hulse-Taylor binary pulsar (at 10^{-4} Hz; Hui et al. 2013), from seismic data of the Earth ($0.05 - 1$ Hz; Coughlin & Harms 2014), and from a pair of torsion-bar antennas (TOBAs; $0.035 - 0.830$ Hz; Shoda et al. 2014). In the $10^{-4} - 10$ Hz regime, in particular, the astrophysical component of the SBGW could well outshine the cosmological component, revealing rich astrophysical information on, for example, the physics of compact objects and star formation history (Regimbau 2011; Schneider et al. 2010; Hils et al. 1990). Proposed space missions to explore the latter frequency range are the New Gravitational wave Observatory NGO (a.k.a. eLISA; Amaro-Seoane et al. 2013) and the DECi-hertz Interferometer Gravitational wave Observatory DECIGO (Kawamura et al. 2011).

Recent theoretical work on the excitation of global stellar oscillations by GWs (Siegel & Roth 2010, 2011) together with helio- and asteroseismic data allows us to employ the Sun and other solar-like stars as astronomical test masses for the detection of GWs. Helioseismic Sun-as-a-star data for internal gravity and pressure modes of the Sun is available from, e.g., the Global Oscillation at Low Frequency (GOLF) instrument aboard the *Solar and Heliospheric Observatory* (*SOHO*) spacecraft (Gabriel et al. 1995), while asteroseismic data from missions like *CoRoT* (Baglin et al. 2006) and *Kepler* (Christensen-Dalsgaard et al. 2009) offer the possibility to employ other solar-like stars.

Here, we propose a method to directly detect or constrain both the astrophysical and cosmological component of the SBGW at mHz and μHz frequencies by using asteroseis-

[1] Max Planck Institute for Gravitational Physics (Albert Einstein Institute), Am Mühlenberg 1, D-14476 Potsdam-Golm, Germany
[2] Kiepenheuer Institut für Sonnenphysik, Schöneckstr. 6, D-79104 Freiburg, Germany

mic observations (Section 2). While this method is general and can be applied to any star, we demonstrate the feasibility of this approach by deducing a direct upper bound around 0.11 mHz using our Sun as a hydrodynamic detector (Section 3). Section 4 is devoted to discussion and conclusions.

2. METHODOLOGY

Our method is based on the theoretical result that stellar oscillations can be excited by an SBGW (Siegel & Roth 2010, 2011). In the case of the Sun, the resulting amplitudes can be close to or comparable with values expected from excitation by near-surface convection (Siegel & Roth 2011), which is considered to be the main driving mechanism for oscillations in the Sun and solar-like stars (e.g., Goldreich & Keeley 1977; Balmforth 1992; Goldreich et al. 1994; Samadi & Goupil 2001; Belkacem et al. 2008). The physical mechanism underlying the excitation by an SBGW is the fact that GWs manifest themselves in oscillating tidal forces: they periodically stretch and compress the spatial dimensions orthogonal to the direction of propagation in a quadrupolar pattern,[3] thus imposing stresses on the matter they pass through. Global stellar oscillations can be classified into acoustic pressure modes (p modes), with pressure gradients as the restoring force, and interior gravity modes (g modes), with buoyancy as the restoring force (Aerts et al. 2010; Unno et al. 1989). Both p and g modes can be excited by GWs, although only quadrupolar eigenmodes can attain non-vanishing amplitudes due to the quadrupole nature of the excitation force. This fact can help to distinguish an SBGW from other excitation mechanisms (the "noise").

The equation of motion for stellar oscillations in presence of external driving by GWs is the inhomogeneous wave equation for the velocity field v (cf. Siegel & Roth 2011)

$$\rho\left(\frac{\partial^2}{\partial t^2} - \mathcal{L}\right)v + \mathcal{D}(v) = \frac{\partial}{\partial t}(f_{\mathrm{Rey}} + f_{\mathrm{entr}} + f_{\mathrm{GW}}), \quad (1)$$

where ρ is the density and $\mathcal{L}$ and $\mathcal{D}$ are linear differential operators (see Siegel & Roth 2011 for definitions). Furthermore, f_{Rey} and f_{entr} denote the Reynold and entropy source terms, respectively, and represent the driving terms due to convective motions (see Siegel & Roth 2011 and Samadi & Goupil 2001 for definitions). In the following, we are solely interested in the driving term due to GWs, f_{GW}, with components given by

$$f_{\mathrm{GW}}^i(x,t) = \frac{1}{2}\rho x^j \frac{\partial^2}{\partial t^2} h^i{}_j. \quad (2)$$

Here, $h_{\mu\nu}$ denotes the GW tensor.[4]

The velocity field in Equation (1) can be expanded in terms of the complete set of eigenfunctions $\{\xi_N(x)\}$ of the operator $\mathcal{L}$, which define the solutions

$$v_{\mathrm{hom}}(x,t) = -\mathrm{i}\omega\xi(x)e^{-\mathrm{i}\omega t} \quad (3)$$

of the homogeneous problem

$$\left(\frac{\partial^2}{\partial t^2} - \mathcal{L}\right)v_{\mathrm{hom}} = 0, \quad (4)$$

$$v(x,t) = \sum_N (-\mathrm{i}\omega_N)A_N(t)\xi_N(x)e^{-\mathrm{i}\omega_N t}. \quad (5)$$

---

[3] This is in general a superposition of the two polarization states of a GW, the cross and plus polarization.

[4] Greek indices take spacetime values 0,1,2,3, whereas Latin indices take spatial values 1,2,3 only. Repeated indices are summed over.

Hence, the intrinsic complex velocity field associated with a stellar oscillation normal mode as a function of time t and position x within the star can be written as

$$v_N(x,t) \equiv -\mathrm{i}\omega_N A_N(t)\xi_N(x)e^{-\mathrm{i}\omega_N t}, \quad (6)$$

where $A_N(t)$ is a time-dependent complex amplitude, $\xi_N(x)$ denotes the displacement eigenfunction, ω_N the oscillation frequency, and $N = (nlm)$ is an abridged index denoting the eigenmode under consideration with radial order n, harmonic degree l and azimuthal order m. In the pulsation frame of a slowly rotating star (polar axis coincides with rotation axis) and spherical coordinates, the displacement eigenfunction can be written as

$$\xi_N(r,\Theta,\Phi) = [\xi_{r,nl}(r)e_r + \xi_{h,nl}(r)r\nabla]Y_{lm}(\Theta,\Phi), \quad (7)$$

which we normalize according to

$$\int_V d^3x\,\rho\xi_N^* \cdot \xi_{N'} = I\delta_{NN'}. \quad (8)$$

In the above equations, $*$ denotes complex conjugation, V the stellar volume, I is a constant that we set to unit mass in cgs units, $\xi_{r,nl}(r)$ and $\xi_{h,nl}(r)$ denote the radial and horizontal eigenfunctions, respectively, and $Y_{lm}(\Theta,\Phi)$ is the spherical harmonic associated with the oscillation mode.

The quantity that is directly accessible to asteroseismic and Sun-as-a-star radial velocity measurements is the disk-integrated, apparent surface velocity of a mode (the observed root mean square (rms) surface velocity), which can be expressed as (cf. also Belkacem et al. 2009; Berthomieu & Provost 1990)

$$v_N = \left\langle \frac{1}{2}|v_{\mathrm{app},N}(R_0,t)|^2 \right\rangle^{1/2}, \quad (9)$$

where $\langle\rangle$ denotes temporal average and where we defined the complex apparent surface velocity

$$v_{\mathrm{app},N}(R_0,t) = \frac{\displaystyle\int_H h(\mu)v_N(x,t)\cdot n\,d\Omega}{\displaystyle\int_H h(\mu)\,d\Omega} \quad (10)$$

as observed in the observer's frame with spherical coordinates (r,θ,ϕ) (the direction $\theta = 0$ points toward the observer and $r = 0$ corresponds to the center of the star). In Equation (10), H denotes the visible half sphere corresponding to the parameter space $\{(\theta,\phi)|0 < \theta < \pi/2,\, 0 < \phi < 2\pi\}$, $\mu = \cos\theta$ the limb angle, $d\Omega = dA \cdot n = R_0^2 \sin\theta\cos\theta d\theta d\phi$ the surface element projected onto the direction of the observer, and R_0 the distance between the center of the star and the layer where the apparent surface velocity is observed. Furthermore, $n = \cos\theta e_r - \sin\theta e_\theta$ is the unit vector at a particular position on H, pointing toward the observer, and $h(\mu)$ is an appropriate limb darkening law. In other words, the apparent surface velocity v_N is the intrinsic line-of-sight velocity at a certain layer in the atmosphere, integrated and weighted over the visible stellar disk according to a certain limb darkening function.

In the case of excitation by an SBGW (i.e., $f_{\mathrm{Rey}} = f_{\mathrm{entr}} \equiv 0$), the intrinsic mean-square amplitude of a quadrupolar ($l = 2$) stellar oscillation mode is time independent and can be directly expressed in terms of the normalized spectral energy

density of the background as (Siegel & Roth 2011):

$$\langle |A_N|^2 \rangle = \frac{\pi^2}{25} \frac{\chi_n^2}{\eta_N \omega_N I^2} H_0^2 \Omega_{\mathrm{GW}}(\omega_N), \qquad (11)$$

where

$$\chi_n = \int_0^R \rho(r) r^3 [\xi_{r,n2}(r) + 3\xi_{h,n2}(r)] \, dr \qquad (12)$$

is part of the coupling factor between the GW field and the stellar oscillation mode. Here, R denotes the stellar radius and η_N is the damping rate associated with mode N. The normalized dimensionless function

$$\Omega_{\mathrm{GW}}(\nu) \equiv \frac{1}{\rho_{\mathrm{crit}}} \frac{d\rho_{\mathrm{GW}}}{d\ln \nu} \qquad (13)$$

is a convenient way of characterizing the properties of an SBGW (Maggiore 2000; Allen & Romano 1999). It measures the energy density of GWs per unit logarithmic frequency interval in units of the present critical energy density, $\rho_{\mathrm{crit}} = 3c^2 H_0^2 / 8\pi G$, that is needed for a closed geometry of the universe. Here, H_0 denotes the present Hubble expansion rate, c the speed of light, and G the gravitational constant.

Furthermore, it can be shown that the intrinsic amplitude A_N is related to v_N as

$$v_N = \frac{1}{\sqrt{2}} \langle |A_N(t)|^2 \rangle^{1/2} \omega_N \Psi_N(R_0), \qquad (14)$$

where

$$\Psi_N(R_0) = |\alpha_{lm} \xi_{r,nl}(R_0) + \beta_{lm} \xi_{h,nl}(R_0)|, \qquad (15)$$

with visibility coefficients

$$\alpha_{lm} = N_{lm} |P_{lm}(\cos\Theta_0)| u_l, \qquad (16)$$
$$\beta_{lm} = N_{lm} |P_{lm}(\cos\Theta_0)| v_l \qquad (17)$$

(cf. also Belkacem et al. 2009; Berthomieu & Provost 1990; Dziembowski 1977; Christensen-Dalsgaard & Gough 1982). Here, $N_{lm} = \sqrt{(2l+1)/4\pi} \sqrt{(l-m)!/(l+m)!}$, P_{lm} denote the associated Legendre polynomials, and

$$u_l = \int_0^1 \tilde{h}(\mu) \mu^2 P_l(\mu) \, d\mu, \qquad (18)$$

$$v_l = l \int_0^1 \tilde{h}(\mu) \mu [P_{l-1}(\mu) - \mu P_l(\mu)] \, d\mu, \qquad (19)$$

with $\tilde{h}(\mu) = h(\mu) / \int_0^1 h(\mu) \mu \, d\mu$ and $P_l = P_{l0}$ the Legendre polynomials.

Given an upper bound on the apparent surface velocity v_N of a quadrupolar stellar eigenmode with frequency $\omega_N = 2\pi\nu_N$ and assuming that the observed oscillations of a star are excited at least partially by a stochastic background of gravitational radiation as one of the driving forces, Equations (11) and (14) imply an upper limit on the normalized spectral energy density of the SBGW according to

$$H_0^2 \Omega_{\mathrm{GW}}(\nu_N) < \frac{25}{\pi^3} \mathcal{X}_N \mathcal{M}_N \frac{\eta_N}{\nu_N} v_N^2. \qquad (20)$$

Here, $\mathcal{X}_N \equiv 1/\chi_n^2$ is the coupling factor between the GW field and the stellar oscillation mode, i.e., the susceptibility of a particular mode to the GW background. The factor

$\mathcal{M}_N \equiv I^2/\Psi_N^2(R_0)$ is the observed mode mass (the observed value for the total interior mass of the star that is affected by the oscillation), which takes instrumental and other observation-related effects into account (cf. Equation (15)). We note that the left-hand side of Equation (20) is independent of the Hubble constant and thus independent of its uncertainty.

3. RESULTS FOR THE SUN

The method described in the previous section is very general and applies to any solar-like oscillator. Here, we compute an upper limit employing our nearest star, the Sun, as a hydrodynamic detector. The underlying solar model that we use is Model S (Christensen-Dalsgaard et al. 1996), which is extensively used as a reference solar model (see, e.g., Turck-Chièze & Couvidat 2011 for a discussion on the current status of the standard solar model). Thanks to the very high level of agreement in the numerical results for solar(-like) models computed with present stellar evolution codes (Lebreton et al. 2008), any other well-fitted solar model could have been used, such as, e.g., the CESAM model employed by Belkacem et al. (2009). We note that the mean quadratic differences in the physical and seismic variables between solar models computed with, e.g., ASTEC and CESAM are particularly small (mean quadratic differences in the physical and thermodynamic variables are often well below or on the order of 1%; differences in the oscillation frequencies are typically less than 0.01%; Lebreton et al. 2008).

The solar oscillation modes best-suited for deducing an upper bound on a GW background are the high-frequency (low radial order) quadrupolar g modes, as they are most sensitive to such a background (Siegel & Roth 2011): the corresponding intrinsic mean-square amplitudes $\langle |A_N|^2 \rangle$ are typically orders of magnitude larger than for low radial order quadrupolar p modes (assuming a constant $\Omega_{\mathrm{GW}}(\nu)$), which is mainly the result of much smaller damping rates (cf. Figure 5 in Siegel & Roth 2011). Combined with the observed much larger surface amplitudes, p modes are less relevant for deducing a tight upper bound on an SBGW and are thus not considered here (note that the upper bound on an SBGW according to Equation (20) scales with the squared surface velocity).

Solar g modes have not been unambiguously detected so far, although some g-mode candidates have been identified in data from the GOLF instrument aboard the *SOHO* spacecraft (Turck-Chièze et al. 2004; García et al. 2007; for a review on quadrupolar p and g-mode measurements, see, e.g., Turck-Chièze & Lopes 2012). Their surface velocities are extremely small, because these modes are evanescent in the convection zone. Theoretical quantitative estimates for solar g-mode surface velocities are highly uncertain and differ from each other by orders of magnitude (e.g., Gough 1985; Bahcall & Kumar 1993; Kumar et al. 1996; Provost et al. 2000; Belkacem et al. 2009), which is predominantly due to the hypotheses made in the excitation models concerning turbulent convection and, in particular, the choice of the eddy-time correlation function (Belkacem et al. 2009). The currently predicted range for quadrupolar g-mode rms surface velocities is $10^{-3} \, \mathrm{mm\,s^{-1}} \lesssim v_N \lesssim 1 \, \mathrm{mm\,s^{-1}}$ (cf. Appourchaux et al. 2010).

Observational upper bounds on g-mode surface amplitudes have been reported numerously in the literature (Appourchaux et al. 2010). As a conservative upper bound on solar g-mode rms surface amplitudes we adopt $6 \, \mathrm{mm\,s^{-1}}$ for

any of the modes (Gabriel et al. 2002), which is the 90% confidence limit deduced from Doppler measurements of the solar disk-integrated line-of-sight velocity field as observed by the GOLF instrument. This limit is based on Level 2 GOLF data, which were calibrated using the method described by Ulrich et al. (2000). Accordingly, we employ for our calculation of visibility coefficients the limb darkening law found by Ulrich et al. (2000),

$$h(\mu) = 1 + c_1(1 - \mu) + c_2(1 - \mu)^2 + c_3(1 - \mu)^3, \quad (21)$$

where $c_1 = -0.466$, $c_2 = -0.06$, and $c_3 = -0.29$. With this limb darkening law, the numerical values for the coefficients u_2 and v_2 (cf. Equations (18) and (19)) are 0.324 and 0.781, respectively. We numerically checked that the precise height in the solar atmosphere where the velocities are observed does not significantly influence our final result. To a very good approximation, we can therefore set $R_0 = R$, where R is the stellar radius. This is to be expected for g modes, given their small amplitudes at the solar surface. The angle between the solar rotation axis and the polar axis of the observer's frame as defined by the position of the *SOHO* spacecraft is $\Theta_0 = 83°$. It is worthwhile to note that the visibility coefficients do not depend on the (time-dependent) azimuthal offset Φ_0 between the pulsation frame and the observer's frame. With these details, the values of the visibility coefficients α_{lm} and β_{lm} (cf. Equations (16) and (17)) can be computed, which we list in Table 1.

A further ingredient are the damping rates. It is important to note that radiative damping is the dominant damping mechanism for asymptotic g modes. Thanks to this fact, g-mode damping rates (excluding the first few radial orders, i.e., at least up to $\approx 110\,\mu$Hz in the case of the Sun) can be reliably calculated with non-adiabatic oscillation computations (Dupret 2002; Belkacem et al. 2009). Above $110\,\mu$Hz, time-dependent convection terms become significant and damping rates are sensitive to the parameter β (cf. Grigahcène et al. 2005) used by Belkacem et al. (2009) to model convection-pulsation interactions. The value adopted by the latter authors was chosen such that good agreement between theoretically computed and observed damping rates of solar p modes was achieved. However, for the lack of corresponding data, this calibration cannot be verified for solar g modes. Although the deviation from the radiative damping power law (see below) will most likely not be large for the first few modes above $110\,\mu$Hz, we cannot entirely trust the upper bounds deduced above this frequency.

Figure 1 shows the upper bounds on an SBGW as deduced from quadrupolar ($l = 2$) asymptotic solar g modes according to Equation (20), in which we have assumed $H_0 = 70\,\mathrm{km\,s^{-1}\,Mpc^{-1}}$ (Komatsu et al. 2011). As can be seen from Figure 1, the upper bounds are tightest at high frequencies and they follow a fairly regular power law, which can be understood from an asymptotic analysis of the quantities appearing in Equation (20). The quantities χ_n^2 and η_N are
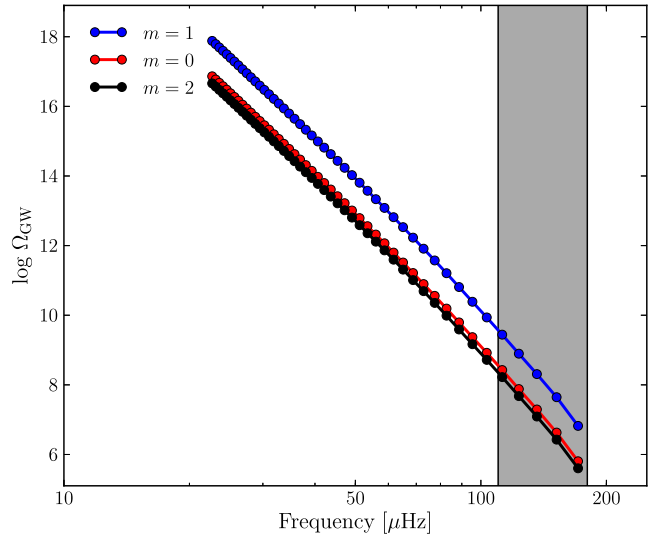

Figure 1. Upper limits on an SBGW from Sun-as-a-star data. The limits shown are deduced from the 90% confidence limit on solar g-mode surface amplitudes (Gabriel et al. 2002) applied to asymptotic quadrupolar modes according to Equation (20) (dots indicate individual modes). Due to visibility effects, the degeneracy in the azimuthal order m is lifted. The frequency regime above $110\,\mu$Hz, where the damping rates cannot be trusted entirely, is indicated in grey (see the text for details).

known to show power-law behavior as a function of frequency for asymptotic g modes (Siegel & Roth 2011; Belkacem et al. 2009). Here, we also find a power law for $\Psi_N^2(R_0)$ in the case of asymptotic g modes. Therefore, according to Equation (20), the upper bound on $\Omega_{\mathrm{GW}}(\nu)$ is also of power-law form. We note that the degeneracy in the azimuthal order m of the modes is lifted due to visibility effects, which are encoded in the quantity $\Psi_N^2(R_0)$ through the visibility coefficients α_{lm} and β_{lm}. The regime above $\approx 110\,\mu$Hz, in which we cannot entirely trust the damping rates (see above), is indicated in gray. The tightest bound that can still be reliably deduced is $\Omega_{\mathrm{GW}} < 1.7 \times 10^8$ at $0.112\,\mathrm{mHz}$, while the tightest overall bound is $\Omega_{\mathrm{GW}} < 4.0 \times 10^5$ at $0.171\,\mathrm{mHz}$. These values are reduced by a factor of four if an upper bound of $3\,\mathrm{mm\,s^{-1}}$ on the apparent g-mode surface velocities according to Turck-Chièze et al. (2004) is used.[5] As evident from Figure 1, the tightest bounds are obtained for g modes with $l = m = 2$, which are compared to other observational constraints on an SBGW in Figure 2. In the latter figure, we mark the former of the aforementioned limits with a large dot.

4. DISCUSSION AND CONCLUSIONS

The frequency range $10^{-4} - 10$ Hz, which is particularly interesting from the astrophysical point of view, has essentially remained unexplored until today in terms of strong bounds. However, several low-frequency antennas are currently being proposed, such as NGO (a.k.a. eLISA), DE-CIGO, or TOBA, with final sensitivities that are claimed to reach $\Omega_{\mathrm{GW}} \sim 10^{-9}$, 10^{-15} and $\Omega_{\mathrm{GW}} \sim 10^{-8}$, respectively (Amaro-Seoane et al. 2013; Kawamura et al. 2011; Ishidoshiro et al. 2011). In this frequency range, cosmological backgrounds (e.g., from cosmic strings) could be outshined by the astrophysical backgrounds from binary neutron stars and galactic as well as extragalactic white dwarfs binaries (Regimbau 2011; Schneider et al. 2010;

Table 1
Values of the Visibility Coefficients (cf. Equations (16) and (17)) for Quadrupolar Modes According to the Limb Darkening Law Equation (21) and an Inclination Angle of $\Theta_0 = 83°$. We note that $\alpha_{2,-m} = \alpha_{2m}$ and $\beta_{2,-m} = \beta_{2m}$.

m	α_{2m}	β_{2m}
0	0.0976	0.235
1	0.0303	0.0729
2	0.123	0.297

[5] Turck-Chièze et al. (2004) estimated the amplitudes of the g-mode candidates they reported to $2 \pm 0.9\,\mathrm{mm\,s^{-1}}$.
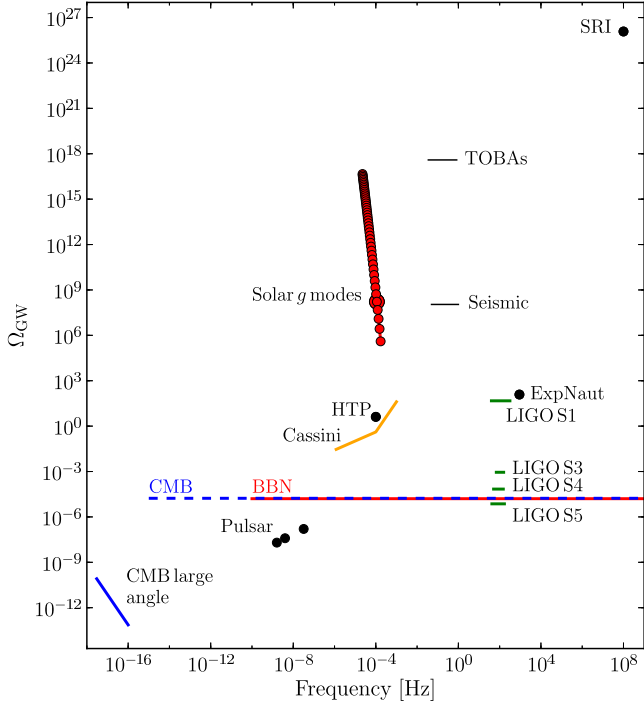
Figure 2. Comparison of present upper bounds on an SBGW and the limits deduced from helioseismic data of the Sun (see the text for details). CMB observations at large angular scales indicate an upper limit on the cosmological component of the SBGW at larger wavelengths than the horizon size at the time of decoupling ($3 \times 10^{-18} - 10^{-16}$ Hz; Maggiore 2000). Pulsar timing observations based on the residuals of the pulse arrival times yield upper bounds between $10^{-9} - 3 \times 10^{-8}$ Hz (Jenet et al. 2006). An upper limit from Doppler tracking of the Cassini spacecraft is obtained in the frequency range $10^{-6} - 10^{-3}$ Hz (Armstrong et al. 2003). Between $0.035 - 0.830$ Hz a pair of TOBAs finds $\Omega_{\mathrm{GW}} < 3.9 \times 10^{17}$ (Shoda et al. 2014), and a pair of synchronous recycling interferometers has placed $\Omega_{\mathrm{GW}} < 1.2 \times 10^{26}$ at 100 MHz (Akutsu et al. 2008). From the variance of orbital elements of the Hulse-Taylor binary pulsar an upper bound roughly one order of magnitude less stringent than the Cassini bound could be deduced at 10^{-4} Hz (Hui et al. 2013). Seismic data of the Earth have recently placed an upper bound of $\Omega_{\mathrm{GW}} < 1.1 \times 10^8$ between $0.05 - 1$ Hz (Coughlin & Harms 2014). A cross-correlation measurement between the Explorer and Nautilus cryogenic resonant bar detectors yielded $\Omega_{\mathrm{GW}} < 122$ at 907.2 Hz (Astone et al. 1999). Also indicated are the upper limits from the S1 to S5 science runs of the Earth-based interferometric detector LIGO around 100 Hz, with the tightest bound being $\Omega_{\mathrm{GW}}(\nu) < 7.3 \times 10^{-6}$ between $41.5 - 169.25$ Hz at 95% confidence (Abbott et al. 2009). Indirect bounds can be deduced from BBN and CMB data (Maggiore 2000; Cyburt et al. 2005; Smith et al. 2006), which constrain the integrated total energy density of the cosmological component of the SBGW in the indicated frequency ranges (see the text for details).

Amaro-Seoane et al. 2013). At lower frequencies where our method can still be applied, the astrophysical background due to supermassive black hole binaries becomes important (e.g., Sesana et al. 2004). The method presented in this paper makes the aforementioned frequency range accessible by providing a possibility to place direct bounds on an SBGW at μHz and mHz frequencies with asteroseismic data. Despite some partial overlap with the Cassini band, this method can somewhat bridge the gap between the Cassini range and the bounds from Earth-based interferometers, possibly improving on the Cassini limits (see below). It is important to point out that there are indirect upper limits in this frequency range, which are deduced from CMB and BBN data due to the fact that a larger amplitude of the SBGW would have altered the observed abundances of the light nuclei created during BBN; analogously, a larger amplitude would have also modified the CMB and matter power spectra. However, these are indirect

bounds in the sense that they constrain the integrated total energy density

$$\Omega_{\mathrm{GW}} = \int \Omega_{\mathrm{GW}}(\nu) d \ln \nu \qquad (22)$$

over the frequency ranges indicated in Figure 2 as $\Omega_{\mathrm{GW,BBN}} < 1.6 \times 10^{-5}$ and $\Omega_{\mathrm{GW,CMB}} < 1.7 \times 10^{-5}$, respectively (Maggiore 2000; Cyburt et al. 2005; Smith et al. 2006). Furthermore, they solely constrain primordial GWs, which already existed at the time when, respectively, the CMB was formed and the nucleosynthesis took place. In particular, these bounds cannot constrain the astrophysically generated GWs, which were produced at later times and which are still generated today. In contrast to these indirect limits, our method reported here yields direct upper bounds that additionally constrain the astrophysical component of the stochastic GW background. They complement the direct upper limits in other frequency bands and the integrated, indirect upper limits in the same frequency regime. Furthermore, unlike most of the other direct bounds, our method does not assume a certain spectral shape for the function $\Omega_{\mathrm{GW}}(\nu)$, i.e., it applies to an arbitrary function $\Omega_{\mathrm{GW}}(\nu)$, regardless of the global shape of $\Omega_{\mathrm{GW}}(\nu)$.

The upper bound given by Equation (20) is highly sensitive to local (i.e., seismic; cf. the wide range in sensitivity in Figures 1 and 2) and global stellar properties and to the observed surface velocities of the modes. Space missions like *CoRoT* and *Kepler* recorded asteroseismic intensity data for a wide range of stellar mass, radius and effective temperature. Furthermore, radial velocity measurements of stellar oscillations from ground exist. The precision of helioseismic measurements might not be achieved by asteroseismology. In particular, from solar observations it can be concluded that the signal-to-noise ratio of intensity variations are expected to be an order of magnitude lower than for velocity measurements (Nigam et al. 1998), and radial velocity measurements might not yet achieve a precision on the order of mm/s. However, these limitations could be overcompensated by several orders of magnitude due to the dependence of Equation (20) on, e.g., stellar mass and radius (Siegel & Roth 2011), and stellar modelling can guide observations to find optimal targets. Still, a conversion from intensity to velocity amplitudes is required before using intensity data in Equation (20), but this might be, e.g., obtained empirically from comparisons of intensity and velocity measurements, as, for instance, carried out by *SOHO* for the Sun (Nigam et al. 1998) or between *Kepler* intensity and follow-up radial velocity data for the stars. Therefore, the existing and up-coming space-based missions, as well as ground-based facilities like SONG (Grundahl et al. 2009), offer a unique possibility to focus on targets with optimized sets of stellar parameters in terms of detector sensitivity and to possibly employ these stars as a large array of low-frequency antennas for the SBGW at μHz and mHz frequencies by using the method presented here.

REFERENCES

Abbott, B. P., the LIGO Scientific Collaboration, & the VIRGO
    Collaboration. 2009, Natur, 460, 990

Aerts, C., Christensen-Dalsgaard, J., & Kurtz, D. W. 2010, Asteroseismology (New York: Springer)

Akutsu, T., Kawamura, S., Nishizawa, A., et al. 2008, PhRvL, 101, 101101

Allen, B., & Romano, J. D. 1999, PhRvD, 59, 102001

Amaro-Seoane, P., Aoudia, S., Babak, S., et al. 2013, GW Notes, 6, 4

Appourchaux, T., Belkacem, K., Broomhall, A.-M., et al. 2010, A&A Rev., 18, 197

Armstrong, J. W., Iess, L., Tortora, P., & Bertotti, B. 2003, ApJ, 599, 806

Astone, P., Bassan, M., Bonifazi, P., et al. 1999, A&A, 351, 811

Baglin, A., Michel, E., Auvergne, M., & The COROT Team. 2006, in ESA Special Publication, Vol. 624, Proc. SOHO 18/GONG 2006/HELAS I, Beyond the spherical Sun, ed. K. Fletcher & M. Thompson (Noordwijk: ESA), 34

Bahcall, J. N., & Kumar, P. 1993, ApJL, 409, L73

Balmforth, N. J. 1992, MNRAS, 255, 639

Belkacem, K., Samadi, R., Goupil, M., & Dupret, M. 2008, A&A, 478, 163

Belkacem, K., Samadi, R., Goupil, M. J., et al. 2009, A&A, 494, 191

Berthomieu, G., & Provost, J. 1990, A&A, 227, 563

Christensen-Dalsgaard, J., Arentoft, T., Brown, T. M., et al. 2009, CoAst, 158, 328

Christensen-Dalsgaard, J., Däppen, W., Ajukov, S. V., et al. 1996, Sci, 272, 1286

Christensen-Dalsgaard, J., & Gough, D. O. 1982, MNRAS, 198, 141

Coughlin, M., & Harms, J. 2014, PhRvL, 112, 101102

Cyburt, R. H., Fields, B. D., Olive, K. A., & Skillman, E. 2005, APh, 23, 313

Dupret, M. A. 2002, BSRSL, 71, 249

Dziembowski, W. 1977, AcA, 27, 203

Gabriel, A. H., Baudin, F., Boumier, P., et al. 2002, A&A, 390, 1119

Gabriel, A. H., Grec, G., Charra, J., et al. 1995, SoPh, 162, 61

García, R. A., Turck-Chièze, S., Jiménez-Reyes, S. J., et al. 2007, Sci, 316, 1591

Goldreich, P., & Keeley, D. A. 1977, ApJ, 212, 243

Goldreich, P., Murray, N., & Kumar, P. 1994, ApJ, 424, 466

Gough, D. O. 1985, in ESA Special Publication, Vol. 235, Future Missions in Solar, Heliospheric and Space Plasma Physics, ed. E. Rolfe & B. Battrick (Noordwijk: ESA Scientific and Technical Publications Branch), 183

Grigahcène, A., Dupret, M., Gabriel, M., Garrido, R., & Scuflaire, R. 2005, A&A, 434, 1055

Grundahl, F., Christensen-Dalsgaard, J., Kjeldsen, H., et al. 2009, in ASP Conf. Ser. 416, Solar-Stellar Dynamos as Revealed by Helio- and Asteroseismology: GONG 2008/SOHO 21, ed. M. Dikpati, T. Arentoft, I. González Hernández, C. Lindsey, & F. Hill (San Francisco, CA: ASP), 579

Hils, D., Bender, P. L., & Webbink, R. F. 1990, ApJ, 360, 75

Hui, L., McWilliams, S. T., & Yang, I.-S. 2013, PhRvD, 87, 084009

Ishidoshiro, K., Ando, M., Takamori, A., et al. 2011, PhRvL, 106, 161101

Jenet, F. A., Hobbs, G. B., van Straten, W., et al. 2006, ApJ, 653, 1571

Kawamura, S., Ando, M., Seto, N., et al. 2011, CQGra, 28, 094011

Komatsu, E., Smith, K. M., Dunkley, J., et al. 2011, ApJS, 192, 18

Kumar, P., Quataert, E. J., & Bahcall, J. N. 1996, ApJL, 458, L83

Lebreton, Y., Montalbán, J., Christensen-Dalsgaard, J., Roxburgh, I. W., & Weiss, A. 2008, Ap&SS, 316, 187

Maggiore, M. 2000, PhR, 331, 283

Nigam, R., Kosovichev, A. G., Scherrer, P. H., & Schou, J. 1998, ApJL, 495, L115

Provost, J., Berthomieu, G., & Morel, P. 2000, A&A, 353, 775

Regimbau, T. 2011, RAA, 11, 369

Samadi, R., & Goupil, M. 2001, A&A, 370, 136

Sathyaprakash, B. S., & Schutz, B. F. 2009, LLR, 12

Schneider, R., Marassi, S., & Ferrari, V. 2010, CQGrav, 27, 194007

Sesana, A., Haardt, F., Madau, P., & Volonteri, M. 2004, ApJ, 611, 623

Shoda, A., Ando, M., Ishidoshiro, K., et al. 2014, PhRvD, 89, 027101

Siegel, D. M., & Roth, M. 2010, MNRAS, 408, 1742

Siegel, D. M., & Roth, M. 2011, ApJ, 729, 137

Smith, T. L., Pierpaoli, E., & Kamionkowski, M. 2006, PhRvL, 97, 021301

Turck-Chièze, S., & Couvidat, S. 2011, RPPh, 74, 086901

Turck-Chièze, S., & Lopes, I. 2012, RRA, 12, 1107

Turck-Chièze, S., García, R. A., Couvidat, S., et al. 2004, ApJ, 604, 455

Ulrich, R. K., Boumier, P., Robillot, J.-M., et al. 2000, A&A, 364, 816

Unno, W., Osaki, Y., Ando, H., Saio, H., & Shibahashi, H. 1989, Nonradial oscillations of stars (2nd edn.; Tokyo: Univ. Tokyo Press)